Brain Imaging and Behavior (2019) 13:933–944
https://doi.org/10.1007/s11682-018-9907-z

ORIGINAL RESEARCH

Claustral structural connectivity and cognitive impairment in drug naïve Parkinson's disease

Alessandro Arrigo[1] · Alessandro Calamuneri[2,3] · Demetrio Milardi[2,4] · Enricomaria Mormina[3,4] · Michele Gaeta[4] · Francesco Corallo[2] · Viviana Lo Buono[2] · Gaetana Chillemi[2] · Silvia Marino[2] · Alberto Cacciola[2,4] · Giuseppe Di Lorenzo[2] · Giuseppina Rizzo[4] · Giuseppe Pio Anastasi[4] · Angelo Quartarone[2,4,5,6]

Published online: 18 June 2018

Abstract

The claustrum is a thin grey matter structure which is involved in a wide brain network. Previous studies suggested a link between claustrum and Parkinson's Disease (PD), showing how α-synuclein pathology may affect claustral neurons as well as how α-synuclein immunoreactivity may correlate with the onset of cognitive dysfunctions. Our aim is to investigate, via diffusion MRI, claustral structural network changes in drug naïve PD patients, with the goal to understand whether such changes may contribute to cognitive decline in PD. 15 drug naïve PD patients and 15 age-matched controls were enrolled; MR protocol was performed on a 3T scanner. Whole brain probabilistic tractography was obtained using Constrained Spherical Deconvolution (CSD) diffusion model. Connectivity matrices were estimated based on a robust anatomical parcellation of structural T1w images. In PD group, impaired subnetworks were correlated with psychological examinations. We found decreased claustral connectivity in PD patients compared to controls, especially with areas mainly involved in visuomotor and attentional systems. Moreover, we found a positive correlation between MoCA and density of pathways connecting ipsilaterally claustrum to left ($r = 0.578$, $p = 0.021$) and right ($r = 0.640$, $p = 0.020$) Pars Orbitalis. Our results support the hypothesis of claustral involvement in cognitive decline in drug naïve PD patients.

Keywords Claustrum · Connectivity · Diffusion MRI · Parkinson's disease · Cognitive assessment; Tractography

Introduction

The histopathological hallmark of both Parkinson's disease (PD) and Lewy Body Dementia (LBD) is the presence of alpha-synuclein (alpha-Syn) positive intraneuronal inclusions known as Lewy bodies and Lewy neurites. Although their presence in the substantia nigra is pathognomonic for PD, alpha-Syn pathological lesions have been reported in several extranigral regions as well. In a very elegant study Kalaitzakis and associates have evaluated the alpha-Syn, tau and amyloid-βeta (Aβ) pathologies in claustrum of 20 PD cases without dementia, 12 PD cases with dementia (PDD) and 7 cases with dementia with LBD (Kalaitzakis et al. 2009). An alpha-Syn positivity has been observed in 75% of PD cases without dementia and in 100% of PDD and LBD cases. On the other hand, Aβ pathology has been observed in claustrum in 25% of PD, 58% of PDD and 100% of LBD cases. The authors concluded that pathology in the claustrum was strongly related to the presence of dementia in PD and LBD.

Claustrum is a thin layer of subcortical gray matter (GM) placed in the deep part of both the cerebral lobes.

Alessandro Arrigo and Alessandro Calamuneri PhD equally contributed to the present work and are considered co-first authors.

Electronic supplementary material The online version of this article (https://doi.org/10.1007/s11682-018-9907-z) contains supplementary material, which is available to authorized users.

✉ Alessandro Calamuneri
alecalamuneri@gmail.com

[1] Department of Ophthalmology, IRCCS Ospedale San Raffaele, University Vita-Salute San Raffaele, Milan, Italy

[2] IRCCS Centro Neurolesi Bonino Pulejo, S.S. 113 – Contrada Casazza, 98124 Messina, Italy

[3] Department of Clinical and Experimental Medicine, University of Messina, Messina, Italy

[4] Department of Biomedical Sciences and Morphological and Functional Images, University of Messina, Messina, Italy

[5] NYU-Langone School of Medicine, New York, NY, USA

[6] The Fresco Institute for Parkinson's & Movement Disorders, New York, NY, USA

Neuroanatomical evidence based on animal studies has demonstrated connections with many neocortical areas including frontal cortex (Kievit and Kuypers 1975), visual cortical fields including striate cortex (Baizer et al. 1997), temporal cortex (Webster et al. 1993), entorhinal cortex (Insausti et al. 1987), parieto-occipital cortex (Shipp et al. 1998) and parietal cortex (Pearson et al. 1982). In addition, claustrum has been shown to be tightly connected to limbic structures such as hippocampus (Amaral and Cowan 1980), amygdala (Amaral and Insausti 1992), caudate nucleus and putamen (Andersen 1968; Arikuni and Kubota 1985). Amygdala, caudate nucleus and putamen regions have been also related to dementia in PD (Ito et al. 2002). In addition, claustral involvement has been reported in LBD, where it has been related to the presence of visual hallucinations (Kosaka 1978; Yamamoto et al. 2007). In Alzehimer's Disease (AD) claustrum has been related to the presence of dementia and cognitive dysfunctions (Morys et al. 1996; Ogomori et al. 1989). In particular, Aβ protein deposits have been extensively found in AD patients, with a predominance of large-sized fibrillary deposits (Ogomori et al. 1989). Neural loss and neurofibrillary tangles observed in the paramygdalar part of the claustrum have led to the hypothesis that claustral Aβ degeneration could be related to the onset and progression of memory dysfunctions and dementia in AD patients (Morys et al. 1996). Anatomical description of neural circuitry has been traditionally provided by axonal tracing studies in non-human primates and by post-mortem fiber dissection in humans. In the last years Diffusion Tensor Imaging (DTI) based tractography has been employed in this research field as an anatomical "virtual dissector". DTI allows indeed to reconstruct in-vivo and non-invasively neural connectivity in human brain (Basser et al. 2000; Mori and van Zijl 2002). By using a more advanced diffusion model, namely Constrained Spherical Deconvolution (CSD), we have shown that claustrum has a widely distributed anatomical network including most of the cortex regions as well as many subcortical structures (Arrigo et al. 2017; Milardi et al. 2015). Our findings have reinforced the idea that claustrum may play a complex physiological role in human brain, as it has been already suggested elsewhere (Torgerson and Van Horn 2014; Torgerson et al. 2015).

In this manuscript, we have evaluated claustrum connectivity profile of a group of drug naïve PD patients and compared it to a healthy age-matched control group, in order to search for meaningful markers of cognitive dysfunction.

Materials and methods

Subject selection and data acquisition

Fifteen PD subjects (mean age 67.93 years, age range = 58–74 years, SD = 4.43 years) were included in the study. They had strictly unilateral symptoms and were treatment-naïve; they satisfied all inclusion and exclusion features of the UK Brain Bank Criteria (Hughes et al. 1992). Furthermore, fifteen age-matched healthy volunteers (mean age 65.33 years, age range = 56–70 years, SD = 4.96 years) were included as a control group. Depression, treatment with antidepressants and bad marker tremor were adopted as exclusion criteria for both groups. Informed consent was obtained from all participants. All procedures were in accordance with the ethical standards of the Ethics Committee of IRCCS Bonino Pulejo, Messina, Italy, and with the 1964 Helsinki declaration and its subsequent amendments or comparable ethical standards. MR acquisition protocol was performed by means of a 3 T Achieva Philips scanner using a 32-channels SENSE head coil (Philips, The Netherlands).

Following MR sequences were acquired:

1. T1 weighted Fast Field Echo (FFE) sequence (TR = 25 ms, TE = 4.6 ms, flip angle = 30°, FOV = 240 × 240 mm^2, reconstruction matrix 240 × 240 voxel, voxel size 1 mm isotropic);
2. A single phase diffusion weighted EPI (DWI) sequence (TR = 11,884 ms, TE = 54 ms, FOV = 240x240mm^2, isotropic 2 mm resolution with any inter-slice gap): it consisted in 61 diffusion weighted directions (b-value 1000s/mm^2), in addition to one un-weighted b0 volume.

Clinical evaluation and cognitive indices

All PD subjects underwent motor subsection of the Unified Parkinson's Disease Rating Scale (UPDRS) (Fahn and Elton 1987) as well as the Hoehn and Yahr scale (HYs) (Hoehn and Yahr 1967). Dementia and depression were assessed using the mini-mental state examination (MMSE) (Folstein et al. 1978) and the Beck's Depression Inventory (BDI) (Beck et al. 1996) respectively. Furthermore, all subjects underwent the Montreal Cognitive Assessment (MoCA) (Nasreddine et al. 2005). Clinical characteristics of all PD patients and controls have been reported in Table 1.

Diffusion pre-processing and co-registration of structural scans

Diffusion data gathered from both groups were corrected for motion as well as for eddy current distortions by means of EDDY FSL command (http://fsl.fmrib.ox.ac.uk/fsl/fslwiki/). At the end of the process, diffusion gradient directions were updated to account for the rotational part of transformation estimated on the diffusion weighted scans. Furthermore, a multiplicative bias field was calculated and applied to DWIs to correct for bias caused by acquisition itself; such bias was estimated by means of FAST FSL tool on the basis of the b0

Table 1 Demographic and clinical data (mean ± SD) of PD patients and healthy controls recruited for the study. Following abbreviations are used: MMSE (Mini Mental State Examination), BDI-II (Beck Depression Inventory - II), UPDRS - score III (Unified Parkinson's Disease Rating Scale – score III)

Demographic and clinical data	PD subjects ($n = 15$)	Controls (n = 15)
Gender (M\F)	8\7	7\8
Age (years)	67.93 (± 4.43)	65.33 (± 4.96)
Age range (years)	58–74	56–70
MMSE	25.73 (± 0.80)	NA
BDI-II	14.87 (± 4.17)	NA
Hoen and Yahr stage	1 (± 0.51)	NA
UPDRS - score III	20.13 (± 1.68)	NA
MoCA	20.6 (± 3.5)	NA

un-weighted images. T1w volumes were subsequently coregistered to DWIs using a non-linear procedure firstly proposed by Besson (Besson et al. 2014). In brief, for each subject, CSF probability maps of both B0 and T1w images were extracted using New Segment SPM8 tool (http://www.fil.ion.ucl.ac.uk/spm/software/spm8/); T1w based CSF probability map was later on warped to match b0 based CSF probability map by means of FLIRT and FNIRT FSL utilities. The combined use of FLIRT and FNIRT has been chosen in accordance with the guidelines reported within the FSL website. Eventually, estimated warping field was applied to T1w volume. We adopted aforementioned non-linear procedure instead of a standard affine transformation to achieve the highest possible overlapping between cortical and subcortical structures in both structural and diffusion spaces.

GM parcellation and claustrum segmentation

For both controls and PD subjects, coregistered T1w images were parcellated using Freesurfer image analysis suit (http://surfer.nmr.mgh.harvard.edu/). Default values of recon-all command were adopted; details of pipeline are described elsewhere, see for instance (Fischl et al. 2004). Desikan-Killiany atlas (Desikan et al. 2006) was chosen to automatically identify cortical GM structures. Sub-cortical segmentation was achieved by means of FIRST FSL tool; compared to Freesurfer sub-cortical segmentation, FIRST was indeed found to provide better results (Smith and Alloway 2010). A total of 84 regions were thus identified and employed for subsequent analyses.

Left and right claustra were manually segmented by an experienced radiologist. For each subject, we searched for possible overlapping between segmented claustra and automatic labelled cortical and sub-cortical areas. This step is of particular relevance considering the close topographical location of claustra to other areas, especially insula cortices and putamen. In two cases, one PD subject and one control, we indeed found a small overlapping fraction of claustra and insula cortices segmentation. Hence, we carefully inspected segmentations and refined automatic parcellation by removing voxels that were erroneously assigned to insula cortices. We were also interested in investigating possible differences between claustra volumes in both groups. To this end, we employed FLIRT and FNIRT utilities to warp T1w volumes into the MNI space. To accomplish this task default options suggested on FSL website were adopted. We used the MNI152_T1_2mm_brain volume available within FSL package as reference.

Diffusion modelling and tractography

CSD model was chosen to fit diffusion signal (Tournier et al. 2007; Tournier et al. 2008): for each voxel, fiber Orientation Distribution Function (fODF) was estimated by means of MRtrix3 package (http://www.mrtrix.org/). Probabilistic whole brain tractography was performed on pre-processed DWIs by generating ten millions streamlines using white matter (WM) mask both as seeding ROI and termination mask. WM masks were segmented based on coregistered T1w volumes by means of New Segment SPM8 functionality. Prior running all computations, WM mask was moderately dilated to allow streamlines to reach GM areas; to this end, *maskfilter* MRtrix3 command was used, setting *npass* option to 1. Specifics of tractographic reconstruction algorithm were the following: ifod2 interpolation scheme, minimal fODF amplitude = 0.15, step size 0.1 mm, maximum angle = 10°.

Connectivity profile extraction and network thresholding

Using MRtrix3 tools we extracted streamlines linking right and left claustra with target ROIs coming from the combined Freesurfer/FIRST parcellation. In this way, we created a structural network underlying connectivity profiles of both right and left claustra. Owing to their proximity with our main structures of interest, connections involving putamen and insula cortices were removed out from the calculations. In this manner we wanted to avoid erroneous density estimations as it was done elsewhere (Torgerson and Van Horn 2014).

To build structural connectograms, two major thresholding criteria had to be defined: the minimal number of streamlines a pathway has to be made of for being considered consistently reconstructed (Digitally Reconstructed Tracts, *DRT*), as well as the minimal number of subjects fulfilling such requirement (subject percentage, *subjperc*). For this study, we considered DRT = 15 and subjperc = 100%. Refer to the discussion section for the rational of those choices.

Statistical analysis

Network analyses

To analyze connectomes we adopted permutation tests. For each network edge representing a connection between either right or left claustra and a given target ROI, a t-statistic *tstat* for independent samples was computed. Subsequently connection densities were randomly shuffled between the two groups and other t-statistics under such null distributions were thus computed. This process was run 5000 times, and the actual *tstat* was evaluated to calculate in which portion of such data driven null distribution it was falling into. Null hypothesis was rejected if *tstat* fell outside 95% of the distribution, thus resulting in an alpha value of 0.05. To account for multiple comparisons issue, Bonferroni degrees of freedom correction was adopted: due to the number of eventually tested connections, our final alpha value was set to $\alpha' = 0.00098$.

A number of factors may influence connectivity analysis: first of all, streamlines were generated in native spaces of the subjects, this making streamlines count dependent on the subjects brain sizes. Furthermore, gender and age differences may explain some of the variability within the data. Thus, before performing permutation tests, a General Linear Model (GLM) was fitted to the data: for each network edge, number of streamlines was used as dependent variable, gender was considered a fixed factor, age and total cranial volumes (TIV) were instead included as covariates. TIVs were added to the model to account for individual differences in brain sizes. For each subject, they were measured by adding up WM, GM and CSF mask volumes obtained by means of New Segment SPM8 toolbox. Subsequently residuals of the fit were retained and fed into the permutation tests. Use of GLM fit to remove confounding factors has been already previously discussed (McNamee 2005); use of GLM residuals to test effect of interest while controlling for covariates has been already introduced in other contexts, like in genetic studies (Lou et al. 2007). GLM fit and permutation tests were carried out using release 2015 of MATLAB software package (www.mathworks.com/products/matlab/). To perform permutation tests a Matlab based implementation was employed (Glerean et al. 2016). It is freely available at http://users.aalto.fi/~eglerean/permutations.html.

Correlation with clinical and cognitive indices

Connections that resulted significantly different between PDs and HVs were correlated with MMSE, UPDRS, HYs, BDI and MoCA scales. For each correlation with a given clinical score we performed a partial correlation, i.e. by controlling for all the other scores. Significance threshold was set to 0.05; no correction for multiple comparisons was applied at this stage.

Of notice, correlations were performed using structural data that were already cleaned for age and gender during network analysis. We however run separate correlation analyses both with and without those covariates to investigate possible influence on our results. We found negligible differences (data not-shown), thus concluding that the pre-whitening step was sufficient to remove out those factors.

The assumptions required for the application of Pearson's correlation coefficient, i.e., normality and homoscedasticity, were fulfilled for all correlations: normality was estimated by means of Komogorov-Smironov tests (data not shown); heteroscedasticity was excluded after careful inspection of scatterplots.

Results

Demographic and clinical data for PD subjects and controls have been reported in Table 1.

In Fig. 1.a we have shown right and left claustra averaged for both PDs (red) and controls (green), overlayed onto a structural T1 volume in MNI space. Claustra volumes, obtained from the warped structural images, were not significantly different between the two groups (average claustral volume controls = 652.70 ± 70.58 mm^3, average claustral volume PD = 621.38 ± 94.13 mm^3, p-value = 0.0621).

In Fig. 1.b we have instead shown an example of the process leading to claustrum connectogram construction in a representative normal subject. On the axial and the top coronal slices the combination of automatic brain parcellation and manual claustral segmentation (blue regions) have been shown. On the coronal view in the bottom part of the panel, claustra connectograms have been further visualized.

Network analysis

In Supplementary Table 1 average connectograms (in percentage) calculated for controls and PD group have been reported, together with their standard deviations.

After applying *DRT* as well as *subjperc* thresholds (see Methods section), 51 connections were investigated. 25 of them were related to the right claustrum, whereas 26 involved the left claustrum. The entire set of connections that underwent statistical analyses has been reported in Supplementary Table 2.

In Table 2 we have reported WM fasciculi showing significant decreased connection density either with right or left claustra in PD group compared to controls. We have observed ipsilateral decreased connection density in PDs between claustra and the following areas: Banks of the superior temporal sulcus (Bankssts), Inferior and Superior Parietal regions, Pars Opercularis and Orbitalis, Postcentral region, Precuneus, Superior Temporal area. Furthermore, decreased connectivity

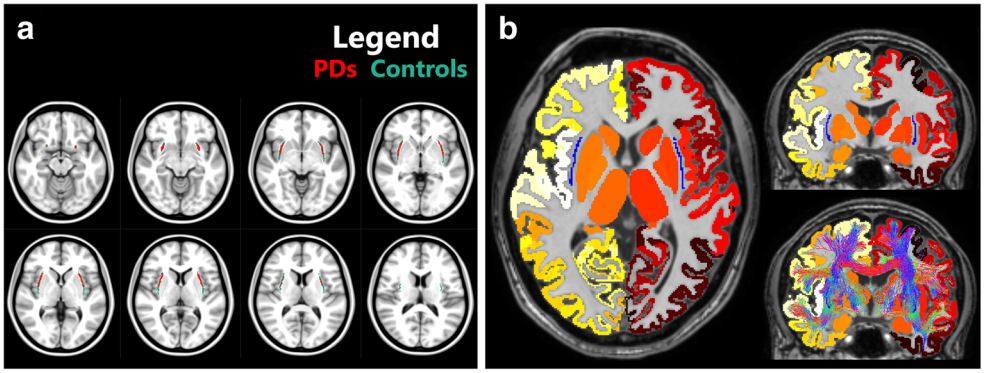

Fig. 1 **a** Left and right claustra, manually segmented, normalized and averaged, are shown superimposed onto a structural image in the MNI space. **b** Structural parcellation of a representative single normal subject. In axial and top coronal slices, blue regions represent claustra. In the bottom coronal view, claustrum connectogram is also shown

has been observed ipsilaterally between right claustrum and Isthmus Cingulate, Middle Temporal gyrus and Pars Triangularis. Decreased density has instead been observed between left claustrum and ipsilateral Precental region. We have not identified WM fasciculi with increased connectivity in the PD group compared to controls. In Fig. 2 we have shown the same results for visualization purposes: in Fig. 2.a we have highlighted links whose density resulted significantly reduced in PD. Each target ROI has been color-coded to ease identification on the Desikan-Killiany atlas, which has been shown from a medial and lateral perspective for both left (Fig. 2.b-d) and right (Fig. 2.c-e) hemispheres respectively.

Table 2 Results of network analyses. Connections with right and left claustra showing statistically significant decreased density in PD group compared to controls are reported. *p*-values are shown (see Methods)

Seed Claustrum Side	Target Side	Target Region	p-values
Left	Left	Bankssts	< 5*10–5
Left	Left	Inferior Parietal	< 5*10–4
Left	Left	Pars Opercularis	< 5*10–4
Left	Left	Pars Orbitalis	< 5*10–4
Left	Left	Postcentral	< 5*10–4
Left	Left	Precuneus	< 5*10–4
Left	Left	Superior Parietal	< 5*10–4
Left	Left	Superior Temporal	< 5*10–4
Left	Left	Precentral	< 5*10–4
Right	Right	Bankssts	< 5*10–5
Right	Right	Inferior Parietal	< 5*10–4
Right	Right	Pars Opercularis	< 5*10–4
Right	Right	Pars Orbitalis	< 5*10–4
Right	Right	Postcentral	< 5*10–4
Right	Right	Precuneus	< 5*10–4
Right	Right	Superior Parietal	< 5*10–4
Right	Right	Superior Temporal	< 5*10–4
Right	Right	Isthmus Cingulate	< 5*10–4
Right	Right	Middle Temporal	< 5*10–5
Right	Right	Pars Triangularis	< 5*10–4

Correlation with cognitive and clinical indices

After controlling for the other scores, we have found bilateral positive correlations between MoCA and Left Pars Orbitalis ($r = 0.578$, uncorrected $p = 0.021$), as well as between MoCA and Right Pars Orbitalis ($r = 0.640$, uncorrected $p = 0.020$). Both correlations have been shown in Fig. 3: in blue, we have reported MoCA of PD subjects against streamlines count connecting right claustrum to right Pars Orbitalis. In red, MoCA scores have been shown against streamlines count linking left claustrum to left Pars Orbitalis. No other significant correlations have been observed.

A MoCA score of 26/30 has been considered the optimal cutoff for Mild Cognitive impairment in PD (PD-MCI), whereas a score below 21/30 hase considered an index for dementia (PD-D) (Dalrymple-Alford et al. 2010). According to this criterion, half of our PD population could be encoded as PD-D (average MoCA = 17.4 ± 1.94, average disease duration = 12.15 ± 5.58 years), whereas the remaining half could be encoded as PD-MCI (average MoCA = 23.17 ± 2.23, average disease duration = 9.85 ± 4.97 years).

Discussion

We have analyzed structural connectivity profiles of right and left claustrum in a group of fifteen drug naïve PD patients. We have found significant changes in comparison to an age-matched healthy population. Moreover, significant correlations with MoCA score have been detected.

Rationale for connectogram thresholding prior to statistical analyses

It is known that diffusion based tractography is prone to false positives; a number of streamlines may thus erroneously connect each claustrum to another target ROIs just by chance or because of reconstruction propagation errors. In order to limit such phenomenon a threshold has to be chosen when building the structural network. Usually, two ROIs are considered to be

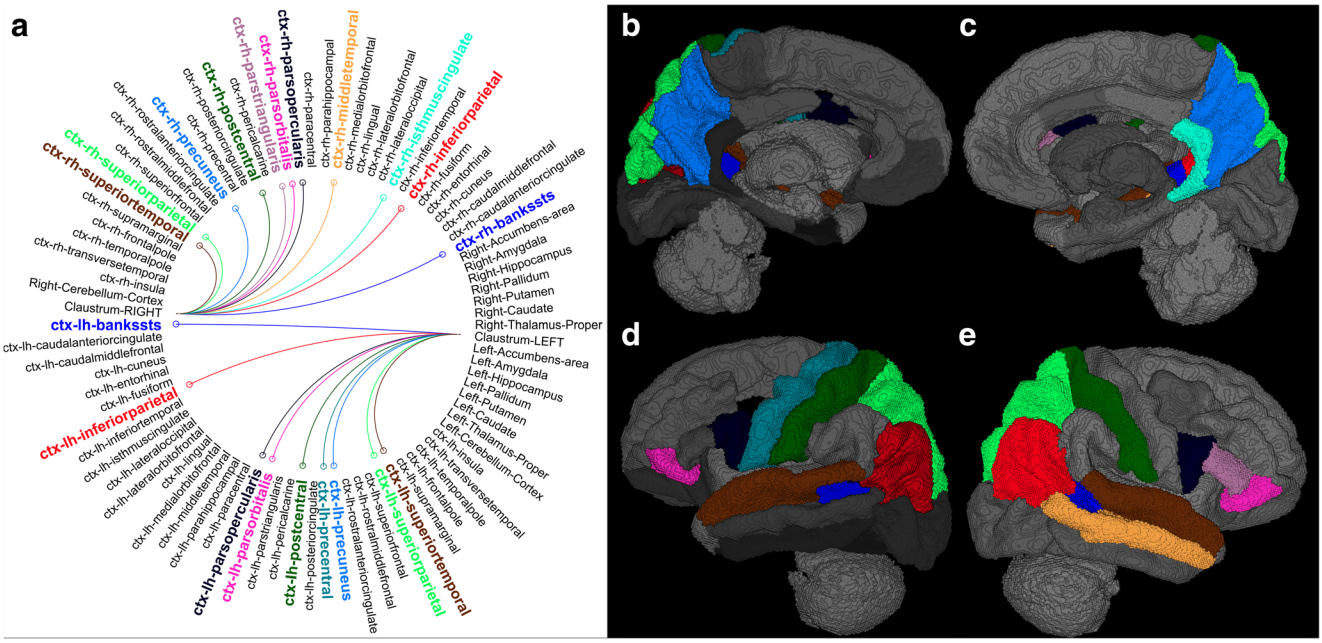

Fig. 2 Results of connectivity analysis. **a** Connectogram showing connections whose density resulted decreased in PD group compared to controls. **b**-**e** Cortical areas, highlighted onto Freesurfer DK atlas template, that have shown decreased connectivity with left (**b**,**c**) and right claustra (**d**,**e**) in PD subjects

linked each other if at least *n* Digitally Reconstructed Tracts (*DRT* = n) connect them. The choice of a proper cutoff is currently matter of debate in related literature (Bullmore and Sporns 2009; Behrens and Sporns 2012; Rubinov and Sporns 2010). In recent clinical oriented articles, no threshold was for instance adopted in a deterministic DTI based network study before creating binary networks (Bijttebier et al. 2015).

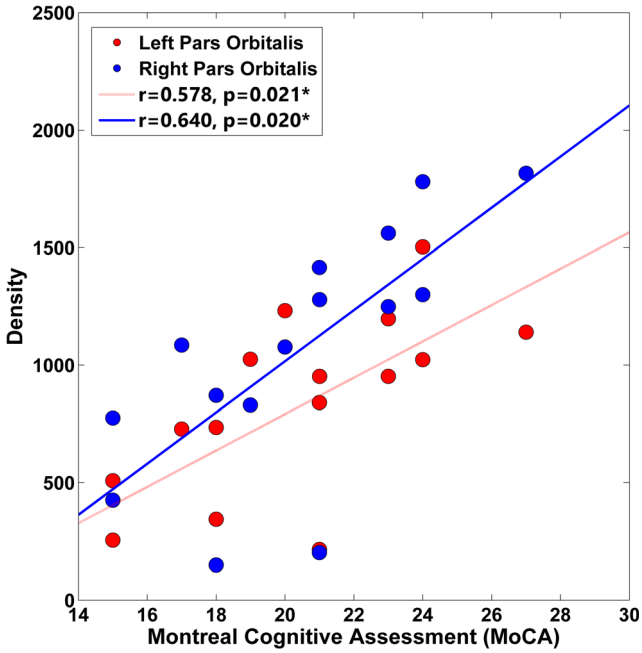

Fig. 3 Correlation between MoCA and connection densities of claustra with ipsilateral Pars Orbitalis. Positive correlation can be observed between both left (red) and right (blue) sides

In (Li et al. 2017) an initial *cutoff* of 3 streamlines was used in a DTI network study of idiopathic Parkinsonians.

In addition, it is a common practice to retain for analyses only connections above the chosen DRT *cutoff* in at least a given subject percentage (*subjperc*). In (Li et al. 2017) *subjperc* was for instance set to 50%, meaning that internodal connections identified in at least half of the patients at the given cutoff were retained.

Since a connection disruption (i.e. DRT = 0) is hard to be robustly demonstrated by means of diffusion MRI because of the actual hardware limitations, we have preferred to avoid inclusion of internodal connections for which a null DRT had been observed in any of the subjects of both groups. In other words, we have set *subjperc* = 100%. In consequence of this choice, our DRT *cutoff* has settled to 15 streamlines, which resulted to be five times more conservative than what was recently done in (Li et al. 2017).

Physiological considerations for healthy group

In keeping with data reported in literature, we have confirmed the existence of a wide claustral network connecting cortical and subcortical brain structures (Crick and Koch 2005; Milardi et al. 2015; Torgerson et al. 2015).

While animal based studies were performed by means of invasive approaches (such as viral tracing ones), in humans similar findings were obtained through non-invasive techniques. In this context, MRI provides a powerful set of tools to carry out both structural and functional investigations (Torgerson and Van Horn 2014). In particular, diffusion MRI

based tractography allows the reconstruction of the most likely WM pathway connecting two GM regions.

Claustral connections have been recently studied, through tractography, by means of both DTI (Torgerson and Van Horn 2014; Torgerson et al. 2015) and CSD (Arrigo et al. 2017; Milardi et al. 2015) diffusion models. CSD (Tournier et al. 2007) has been shown to provide highly accurate results for applications in clinical settings (Farquharson et al. 2013; Tournier et al. 2008), both in healthy and pathological conditions (Arrigo et al. 2014; Arrigo et al. 2016; Milardi et al. 2015; Mormina et al. 2015a, b; Cacciola et al. 2016; Cacciola et al. 2017).

Crick and Koch (Crick and Koch 2005) compared claustrum to an orchestra conductor coordinating a group of players (the various cortical regions). This metaphor is in keeping with the fascinating idea that the different attributes of a given object, both within (e.g., color and motion) and across modalities (e.g., visual form and sound location), are rapidly brought together and integrated into the claustrum (Crick and Koch 2005). Claustrum has been indeed suggested to be involved in several neural functions, including consciousness (Crick and Koch 2005), visual functions (LeVay and Sherk 1981; Sherk and LeVay 1981), auditory functions (Remedios et al. 2014) and motor control (Shima et al. 1996; Tanné-Gariépy et al. 2002).

The highly dense connectivity profiles that were observed in the present study (Fig. 1) are in keeping with the previous findings. They confirm the view of claustrum as an integrator of multimodal aspects of brain functions (Smith and Alloway 2010; Remedios et al. 2014; Edelstein and Denaro 2004; Naghavi et al. 2007; Smith and Alloway 2014; Smythies et al. 2012).

Claustral network in PD

We have not detected significant claustral atrophy in PD group when a direct comparison with controls has been performed. To the best of our knowledge, few studies reporting volumetric analysis of claustrum in PD have been conducted. A previous study by Shao et al. (2015) described a different behavior of claustral volumetric alterations in PD and Parkinson variant of multiple system atrophy (MSA-P), with respect to healthy controls, considering both relatively early stages and more advanced ones. These authors reviewed several studies assessing claustral atrophic phenomena occurring in these pathologic conditions. They reported significant claustral GM reduction in MSA-P patients with at least five years of disease's duration, without however significant claustral volumetric changes in PD. Atrophic claustral and insular alterations have been previously associated with the progressive development of cognitive impairment and dementia. These GM alterations have been suggested to be used as possible predictive biomarkers of the onset of cognitive downfall (Roquet et al. 2017). The cognitive decline in PD may follow different patterns. For example, increased cognitive alterations have been observed in non-tremor dominant PD subjects compared to tremor ones (Selikhova et al. 2009; Lewis et al. 2005). Such aspect has been primarily linked to alpha-Syn aggregates, even if other protein aggregates have been found to correlate with PD (Kalia and Lang 2015). In a recent study by Rektor et al. (2018), widespread WM alterations could be observed in PD patients without cognitive impairment. Since those pathological changes precede GM atrophy, those authors suggested that WM alterations could be used to predict neuronal loss in the corresponding GM regions. Taking into account all these considerations, our data are in agreement with previous studies and may further reinforce the hypothesis that atrophy occurs at later stages of the disease, especially when cognitive decline is more prominent (Kalia and Lang 2015). However, most of the studies available in literature on this topic, including the present one, were designed as cross-sectional investigations or included a relatively short follow-up. For this reason, further larger prospective studies should be conducted in order to confirm these speculations. On the other hand, we cannot exclude that a lack of statistical power might contribute to explain our result. For this reason as well, further studies exploring claustral volumetric differences between PD subgroups on larger populations are needed.

We have found significant alterations of claustral structural network in PD patients (see Table 2). To the best of our knowledge, this is the first investigation of structural claustral connectivity in PD. Even if claustral white matter pathways have not been systematically evaluated in PD patients, there is evidence that alpha-Syn pathology may involve claustrum (Jellinger 2009; Compta et al. 2011). It has been indeed demonstrated that claustrum is positive to alpha-Syn immunoreactive astrocytes (Braak et al. 2007), and that it highly expresses alpha-Syn related gene (Liscovitch and French 2014). Alpha-Syn related damage was positively correlated to the onset of visual hallucinations as well as to the development of cognitive dysfunctions, even if claustrum resulted to be affected by alpha-Syn deposits also in PD patients without dementia (Yamamoto et al. 2007; Kamagata et al. 2012).

Claustral connectivity patterns reported in the literature involve frontal, temporal and entorhinal cortices, as well as hippocampus, thalamus, amygdala, caudate nucleus and putamen. Such patterns place claustrum in a neuroanatomical circuitry relevant in cognitive functions.

Attentional dysfunctions were indeed linked with specific retinopathy, deficits in the primary visual pathway and the secondary ventral and dorsal pathways (Diederich et al. 2014). Visual deficit and attentional dysfunction together were posited as the causes of erroneous 'guess' localization of visual stimuli, poor saccades and motion perception, as well as poor emotional face perception with blunted autonomic reaction (Diederich et al. 2014). This symptoms constellation

might be due to an abnormal cerebral activity in the claustrum (Smythies 2015).

The decreased connectivity that we have observed with cingulum might be related to the possible onset of cognitive dysfunction. It has been indeed reported that alterations of cingulate pathways occur in PD both with and without dementia, even if a larger reduction has been linked to the development of noticeable cognitive impairment (Kamagata et al. 2012). Functional studies dedicated to the cingulum have supported the hypothesis of cingulate alterations occurring in both patterns of PD, thus suggesting that different damage combinations might happen in PD patients and might justify clinical heterogeneity (Camicioli et al. 2004; Mito et al. 2005).

Moreover, we have observed significant decreased claustral connectivity with precuneus. This result is in accordance with an article in which the hypofunction of precuneus has been related to memory and executive tasks alterations in PD (Dušek et al. 2012). Such alteration might also contribute to explain poor visuospatial processing (Filoteo et al. 2014) that may prelude to dementia and visual hallucinations previously reported in PD (Kalaitzakis et al. 2009). Several studies have further shown that precuneus is strongly involved in visuomotor processing and learning (Kawashima et al. 1995; Parsons et al. 2005; Culham et al. 2006).

In addition to parieto-temporal changes, visual hallucinations have been linked to default mode network dysfunction (Yao et al. 2014), which in turn have been correlated with saccadic accuracy (Gorges et al. 2013). Since claustrum has been found to superintend to the control of saccadic movements (Smith and Alloway 2014), it might be hypothesized that claustral connectivity alterations in visual areas as well in regions involved in visuomotor control account for the impairment within the default mode network.

Parietal and temporal connectivity alterations in early PD have been related to cognitive and default mode network dysfunctions (Martin et al. 2009; van Eimeren et al. 2009). Our findings of altered claustral connections with those regions might further support those findings.

It is worthy to note that significant connectivity changes resulted bilaterally distributed except for Precentral, Isthmus Cingulate, Middle Temporal and Pars Triangularis regions. Since all patients were right-handed, this different distribution of connectivity alterations might be related to the left cortical dominance, therefore justifying left alterations for a motor structure (Precentral) and right ones for brain regions dedicated to language and memory functions.

Despite none of our patients complained any disperceptive visual symptom, it would be interesting in a follow up study to see whether changes in the claustro-visuomotor network may predict the development of future visual hallucinations.

Possible markers of cognitive dysfunction in drug naïve PD

We have detected decreased claustral connectivity with Pars Orbitalis and Pars Opercularis. Those structures have already been found altered in previous studies performed in PD subjects without dementia. They have moreover been found to be linked to the following cognitive dysfunctions: poor inhibitory control, bad verbal fluency, poor visuo-constructive ability and poor memory performance (Filoteo et al. 2014; Chen et al. 2015).

Cognitive impairment with and without dementia is an increasingly recognized non-motor complication of PD with significant clinical impact (Poewe 2008; Simuni & Sethi 2008; Meireles and Massano 2012). Interestingly, we have found in PD a positive correlation between MoCA and claustrum connection profile with ipsilateral Pars Orbitalis. It is however worth to mention that no correction for multiple comparison has been adopted at this stage. To the best of our knowledge, this is the first work linking structural connectivity of claustra in PD with cognitive decline.

MoCA has been designed as a rapid screening instrument in PD to detect mild cognitive impairment (PD-MCI) and PD dementia (Fengler et al. 2016). It assesses different cognitive domains: visuospatial/executive (5 points), naming (3 points), attention (6 points), language (3 points), abstraction (2 points), memory (5 points), and orientation (6 points). MoCA has been already used as covariate in a previous fMRI study showing that Pars Opercularis and Pars Triangularis are altered in PD (Nombela et al. 2014). MoCA effectiveness for evaluating cognitive impairment has been already previously reported in different conditions (Trzepacz et al. 2015; Roalf et al. 2013; Fiorenzato et al. 2016) including PD (Biundo et al. 2016).

Although correlation does not imply causation, our results may reinforce the view of Pars Orbitalis and Pars Opercularis as important regions for cognitive control and suggest that the claustrum and its connections may play a relevant role for cognitive impairment in PD (Chaudhuri and Schapira 2009; Huang et al. 2007).

We have not found significant correlation between claustral connection densities and other cognitive indices, like MMSE. A possible explanation for that might be found in the lack of statistical power due to the relative small sample size. Another possible explanation might be related to the higher sensitivity of MoCA if compared to, e.g., MMSE (Biundo et al. 2016).

Limitations and conclusion

Considering the small sample size, further studies are needed to correlate claustral network damages with disease progression, as well as with possible effects of pharmacological treatments.

In addition, it is worth to notice that correction for multiple comparisons has been applied to identify an impaired subnetwork in PD group. However, it has not been applied when making correlations with clinical data. This last aspect has to be carefully taken into account; further studies are needed to challenge the results obtained in this manuscript.

As stated in results section, half of our PD population could be encoded as PD-D (those with a MoCA score not below 26/30), while the remaining half could be encoded as PD-MCI (those with a MoCA score below 21/30, see Fig. 3). Due to the small sample size, we could not run neither separate analyses nor compare those two subgroups. However, from the trend observed in our data (see, for instance, the correlation with Pars Orbitalis in Fig. 3), two different patterns between PD-D and PD-MCI seem not to occur. Further studies involving bigger populations will be however necessary to dispute this hypothesis.

Compliance with ethical standards

Conflict of interest The authors declare that they have no conflict of interest.

References

Amaral, D. G., & Cowan, W. M. (1980). Subcortical afferents to the hippocampal formation in the monkey. *The Journal of Comparative Neurology, 189*, 573–591. https://doi.org/10.1002/cne.901890402.

Amaral, D. G., & Insausti, R. (1992). Retrograde transport of D-[3H]-aspartate injected into the monkey amygdaloid complex. *Experimental Brain Research, 88*(2), 375–388.

Andersen, D. L. (1968). Some striatal connections to the claustrum. Experimental Neurology, 20(2):261-267 https://doi.org/10.1016/0014-4886(68)90100-3, 267.

Arikuni, T., & Kubota, K. (1985). Claustral and amygdaloid afferents to the head of the caudate nucleus in macaque monkeys. *Neuroscience Research, 2*(4), 239–254.

Arrigo, A., Mormina, E., Anastasi, G. P., Gaeta, M., Calamuneri, A., Quartarone, A., De Salvo, S., Bruschetta, D., Rizzo, G., Trimarchi, F., & Milardi, D. (2014). Constrained spherical deconvolution analysis of the limbic network in human, with emphasis on a direct cerebello-limbic pathway. *Frontiers in Human Neuroscience, 8*, 987. https://doi.org/10.3389/fnhum.2014.00987.

Arrigo, A., Calamuneri, A., Mormina, E., Gaeta, M., Quartarone, A., Marino, A., Anastasi, G. P., & Aragona, P. (2016). New insights in the optic radiations connectivity in the human brain. *Investigative Ophthalmology & Visual Science, 57*(1), 1–5. https://doi.org/10.1167/iovs.15-18082.

Arrigo, A., Mormina, E., Calamuneri, A., Gaeta, M., Granata, F., Marino, S., Anastasi, G. P., & Quartarone, A. (2017). Inter-hemispheric Claustral connections in human brain: A constrained spherical deconvolution-based study. *Clinical Neuroradiology, 27*, 275–281. https://doi.org/10.1007/s00062-015-0492-x.

Baizer, J. S., Lock, T. M., & Youakim, M. (1997). Projections from the claustrum to the prelunate gyrus in the monkey. *Experimental Brain Research, 113*, 564–568.

Basser, P. J., Pajevic, S., Pierpaoli, C., Duda, J., & Aldroubi, A. (2000). In vivo fiber tractography using DT-MRI data. *Magnetic Resonance in Medicine, 44*, 625–632.

Beck, A. T., Steer, R. A., Brown, G. K. (1996). Manual for the Beck Depression Inventory-II. San Antonio, TX. 1996: *Psychological Corporation*.

Behrens, T. E., & Sporns, O. (2012). Human connectomics. *Current Opinion in Neurobiology, 22*(1), 144–153. https://doi.org/10.1016/j.conb.2011.08.005.

Besson, P., Dinkelacker, V., Valabregue, R., Thivard, L., Leclerc, X., Baulac, M., Sammler, D., Colliot, O., Lehéricy, S., & Samson, D. S. (2014). Structural connectivity differences in left and right temporal lobe epilepsy. *NeuroImage, 100*, 135–144. https://doi.org/10.1016/j.neuroimage.2014.04.071.

Bijttebier, S., Caeyenberghs, K., van den Ameele, H., Achten, E., Rujescu, D., Titeca, K., & Van Heeringen, C. (2015). The vulnerability to suicidal behavior is associated with reduced connectivity strength. *Frontiers in Human Neuroscience, 9*, 632. https://doi.org/10.3389/fnhum.2015.00632.

Biundo, R., Weis, L., Bostantjopoulou, S., Stefanova, E., Falup-Pecurariu, C., Kramberger, M. G., Geurtsen, G. J., Antonini, A., Weintraub, D., & Aarsland, D. (2016). MMSE and MoCA in Parkinson's disease and dementia with Lewy bodies: A multicenter 1-year follow-up study. *Journal of Neural Transmissions (Vienna), 123*(4), 431–438. https://doi.org/10.1007/s00702-016-1517-6.

Braak, H., Sastre, M., & Del Tredici, K. (2007). Development of alpha-synuclein immunoreactive astrocytes in the forebrain parallels stages of intraneuronal pathology in sporadic Parkinson's disease. *Acta Neuropathologica, 114*(3), 231–241.

Bullmore, E., & Sporns, O. (2009). Complex brain networks: Graph theoretical analysis of structural and functional systems. *Nature Reviews Neuroscience, 10*, 186–198.

Cacciola, A., Milardi, D., Anastasi, G. P., Basile, G. A., Ciolli, P., Irrera, M., Cutroneo, G., Bruschetta, D., Rizzo, G., Mondello, S., Bramanti, P., & Quartarone, A. (2016). A directo Cortico-Nigral pathway as revealed by constrained spherical deconvolution Tractography in humans. *Frontiers in Human Neuroscience, 10*. https://doi.org/10.3389/fnhum.2016.00374.

Cacciola, A., Calamuneri, A., Milardi, D., Mormina, E., Chillemi, G., Marino, S., Naro, A., Rizzo, V., Anastasi, G. P., & Quartarone, A. (2017). A Connectomic analysis of the human basal ganglia network. *Frontiers in Neuroanatomy, 11*, 85. https://doi.org/10.3389/fnana.2017.00085.

Camicioli, R. M., Korzan, J. R., Foster, S. L., Fisher, N. J., Emery, D. J., Bastos, A. C., & Hanstock, C. C. (2004). Posterior cingulate metabolic changes occur in Parkinson's disease patients without dementia. *Neuroscience Letters, 354*(3), 177–180.

Chaudhuri, K. R., & Schapira, A. H. (2009). Non-motor symptoms of Parkinson's disease: Dopaminergic pathophysiology and treatment. *Lancet Neurology, 8*(5), 464–474. https://doi.org/10.1016/S1474-4422(09)70068-7.

Chen, Y., Pressman, P., Simuni, T., Parrish, T. B., & Gitelman, D. R. (2015). Effects of acute levodopa challenge on resting cerebral blood flow in Parkinson's disease patients assessed using pseudo-continuous arterial spin labeling. *PeerJ, 3*, e1381. https://doi.org/10.7717/peerj.1381.

Compta, Y., Parkkinen, L., O'sullivan, S. S., Vandrovcova, J., Holton, J. L., Collins, C., Lashley, T., Kallis, C., Williams, D. R., & de Silva, R. (2011). Lewy-and Alzheimer-type pathologies in Parkinson's disease dementia: Which is more important? *Brain, 134*(5), 1493–1505. https://doi.org/10.1093/brain/awr031.

Crick, F. C., & Koch, C. (2005). What is the function of the claustrum? *Philosophical Transaction of the Royal Society B Biological, 360*(1458), 1271–1279. https://doi.org/10.1098/rstb.2005.1661.

Culham, J. C., Cavina-Pratesi, C., & Singhal, A. (2006). The role of parietal cortex in visuomotor control: What have we learned from neuroimaging? *Neuropsychologia, 44*(13), 2668–2684.

Dalrymple-Alford, J. C., MacAskill, M. R., Nakas, C. T., Livingston, L., Graham, C., Crucian, G. P., Melzer, T. R., Kirwan, J., Keenan, R., Wells, S., Porter, R. J., Watts, R., & Anderson, T. J. (2010). The MoCA well-suited screen for cognitive impairment in Parkinson disease. *Neurology, 75*(19), 1717–1725.

Desikan, R. S., Ségonne, F., Fischl, B., Quinn, B. T., Dickerson, B. C., Blacker, D., Buckner, R. L., Dale, A. M., Maguire, R. P., Hyman, B. T., Albert, M. S., & Killiany, R. J. (2006). An automated labeling system for subdividing the human cerebral cortex on MRI scans into gyral based regions of interest. *NeuroImage, 31*(3), 968–980. https://doi.org/10.1016/j.neuroimage.2006.01.021.

Diederich, N. J., Stebbins, G., Schiltz, C., & Goetz, C. G. (2014). Are patients with Parkinson's disease blind to blindsight? *Brain, 137*, 1838–1849. https://doi.org/10.1093/brain/awu094.

Dušek, P., Jech, R., Sieger, T., Vymazal, J., Růžička, E., Wackermann, J., & Mueller, K. (2012). Abnormal activity in the precuneus during time perception in Parkinson's disease: An fMRI study. *PLoS One, 7*(1), e29635. https://doi.org/10.1371/journal.pone.0029635.

Edelstein, L. R., & Denaro, F. J. (2004). The claustrum: A historical review of its anatomy, physiology, cytochemistry and functional significance. *Cellular and molecular biology (Noisy-le-grand), 50*(6), 675–702.

Fahn, S., Elton, R. L. (1987) and Members od UPDRS Development Committee. The Unified Parkinson's Disease Rating Scale. In: Fahn S, Marsden CD, Calne DB, Goldstein M, editors. Recent Developments in Parkinson's Disease, Macmillan Healthcare Information; Florham Park. p.153–163.

Farquharson, S., Tournier, J. D., Calamante, F., Fabinyi, G., Schneider-Kolsky, M., Jackson, G. D., & Connelly, A. (2013). White matter fiber tractography: Why we need to move beyond DTI: Clinical article. *Journal of Neurosurgery, 118*(6), 1367–1377. https://doi.org/10.3171/2013.2.JNS121294.

Fengler, S., Kessler, J., Timmermann, L., Zapf, A., Elben, S., Wojtecki, L., Tucha, O., & Kalbe, E. (2016). Screening for cognitive impairment in Parkinson's disease: Improving the diagnostic utility of the MoCA through subtest weighting. *PLoS One, 11*(7), e0159318. https://doi.org/10.1371/journal.pone.0159318.

Filoteo, J. V., Reed, J. D., Litvan, I., & Harrington, D. L. (2014). Volumetric correlates of cognitive functioning in nondemented patients with Parkinson's disease. *Movement Disorders, 29*(3), 360–367. https://doi.org/10.1002/mds.25633.

Fiorenzato, E., Weis, L., Falup-Pecurariu, C., Diaconu, S., Siri, C., Reali, E., Pezzoli, G., Bisiacchi, P., Antonini, A., & Biundo, R. (2016). Montreal cognitive assessment (MoCA) and mini-mental state examination (MMSE) performance in progressive supranuclear palsy and multiple system atrophy. *Journal of Neural Transmission, 123*, 1435–1442. https://doi.org/10.1007/s00702-016-1589-3.

Fischl, B., van der Kouwe, A., Destrieux, C., Halgren, E., Sègonne, F., Salata, D. H., Busa, E., Seidman, L. J., Goldstein, J., Kennedy, D., Caviness, V., Makris, N., Rosen, B., & Dale, A. M. (2004). Automatically Parcellating the human cerebral cortex. *Cerebral Cortex, 14*, 11–22.

Folstein, M. F., Folstein, S. E., & McHugh, P. R. (1978). Mini-mental state. A practical method for grading the cognitive state of patients for the clinician. *Journal of Psychiatric Research, 12*(3), 189–198.

Glerean, E., Pan, R. K., Salmi, J., Bernard, B., Merkitch, D., deToledo-Morrell, L., & Goetz, C. G. (2016). Reorganization of functionally connected brain subnetworks in high-functioning autism. *Human Brain Mapping, 37*, 1066–1079.

Gorges, M., Müller, H. P., Lulé, D., Ludolph, A. C., Pinkhardt, E. H., & Kassubek, J. (2013). Functional connectivity within the default mode network is associated with saccadic accuracy in Parkinson's disease: A resting-state FMRI and videooculographic study. *Brain Connectivity, 3*(3), 265–272. https://doi.org/10.1089/brain.2013.0146.

Hoehn, M. M., & Yahr, M. D. (1967). Parkinsonism: Onset, progression, and mortality. *Neurology, 17*, 427–442.

Huang, C., Tang, C., Feigin, A., Lesser, M., Ma, Y., Pourfar, M., Dhawan, V., & Eidelberg, D. (2007). Changes in network activity with the progression of Parkinson's disease. *Brain, 130*(Pt 7), 1834–1846.

Hughes, A. J., Daniel, S. E., Kilford, L., & Lees, A. J. (1992). Accuracy of clinical diagnosis of idiopathic Parkinson's disease: A clinico-pathological study of 100 cases. *Journal of Neurology, Neurosurgery and Psychiatry, 55*(3), 181–184.

Insausti, R., Amaral, D. G., & Cowan, W. M. (1987). The entorhinal cortex of the monkey: III. Subcortical afferents. *The Journal of Comparative Neurology, 264*, 396–408.

Ito, K., Nagano-Saito, A., Kato, T., Arahata, Y., Nakamura, A., Kawasumi, Y., Hatano, K., Abe, Y., Yamada, T., Kachi, T., & Brooks, D. J. (2002). Striatal and extrastriatal dysfunction in Parkinson's disease with dementia: A 6-[18F]fluoro-l-dopa PET study. *Brain, 125*(6), 1358–1365. https://doi.org/10.1093/brain/awf134.

Jellinger, K. A. (2009). A critical evaluation of current staging of alpha-synuclein pathology in Lewy body disorders. *Biochimica et Biophysica Acta, 1792*(7), 730–740. https://doi.org/10.1016/j.bbadis.2008.07.006.

Kalaitzakis, M. E., Pearce, R. K. B., & Gentleman, S. M. (2009). Clinical correlates of pathology in the claustrum in Parkinson's disease and dementia with Lewy bodies. *Neuroscience Letters, 461*(1), 12–15. https://doi.org/10.1016/j.neulet.2009.05.083.

Kalia, L. V., & Lang, A. E. (2015). Parkinson's disease. *The Lancet, 386*(9996), 896–912. https://doi.org/10.1016/S0140-6736(14)61393-3.

Kamagata, K., Motoi, Y., Abe, O., Shimoji, K., Hori, M., Nakanishi, A., Sano, T., Kuwatsuru, R., Aoki, S., & Hattori, N. (2012). White matter alteration of the cingulum in Parkinson disease with and without dementia: Evaluation by diffusion tensor tract-specific analysis. *American Journal of Neuroradiology, 33*(5), 890–895. https://doi.org/10.3174/ajnr.A2860.

Kawashima, R., Roland, P. E., & O'Sullivan, B. T. (1995). Functional anatomy of reaching and visuomotor learning: A positron emission tomography study. *Cerebral Cortex, 5*(2), 111–122.

Kievit, J., & Kuypers, H. G. (1975). Subcortical afferents to the frontal lobe in the rhesus monkey studied bymeans of retrograde horseradish peroxidase transport. *Brain Research, 85*, 261–266.

Kosaka, K. (1978). Lewy bodies in cerebral cortex, report of three cases. *Acta Neuropathologica, 42*, 127–134.

LeVay, S., & Sherk, H. (1981). The visual claustrum of the cat. I. Structure and connections. *Journal of Neuroscience, 1*(9), 956–980.

Lewis, S. J. G., Foltynie, T., Blackwell, A. D., Robbins, T. W., Owen, A. M., & Barker, R. A. (2005). Heterogeneity of Parkinson's disease in the early clinical stages using a data driven *Approach*. *Journal of Neurology, Neurosurgery & Psychiatry, 76*(3), 343–348. https://doi.org/10.1136/jnnp.2003.033530.

Li, C., Huang, B., Zhang, R., Ma, Q., Yang, W., Wang, L., Wang, L., Xu, Q., Feng, J., Liu, L., Zhang, Y., & Huang, R. (2017). Impaired topological architecture of brain structural networks in idiopathic Parkinson's disease: A DTI study. *Brain Imaging and Behavior, 11*(1), 113–128. https://doi.org/10.1007/s11682-015-9501-6.

Liscovitch, N., & French, L. (2014). Differential co-expression between α-Synuclein and IFN-γ signaling genes across development and in Parkinson's disease. *PLoS One, 9*(12), e115029. https://doi.org/10.1371/journal.pone.0115029.

Lou, X. Y., Chen, G. B., Yan, L., Ma, J. Z., Zhu, J., Elston, R. C., & Li, M. D. (2007). A generalized combinatorial approach for detecting Gene-by-gene and gene-by-environment interactions with application to nicotine dependence. *American Journal of Human Genetics, 80*, 1125–1137.

Martin, W. R., Wieler, M., Gee, M., & Camicioli, R. (2009). Temporal lobe changes in early, untreated Parkinson's disease. *Movement Disorders, 24*(13), 1949–1954. https://doi.org/10.1002/mds.22680.

McNamee, R. (2005). Regression modelling and other methods to control confounding. *Occupational and Enviromental Medicine, 62*, 500–506.

Meireles, J., & Massano, J. (2012). Cognitive impairment and dementia in Parkinson's disease: Clinical features, diagnosis, and management. *Frontiers in Neurology, 3*. https://doi.org/10.3389/fneur.2012.00088.

Milardi, D., Bramanti, P., Milazzo, C., Finocchio, G., Arrigo, A., Santoro, G., Trimarchi, F., Quartarone, A., Anastasi, G., & Gaeta, M. (2015). Cortical and subcortical connections of the human claustrum revealed in vivo by constrained spherical deconvolution tractography. *Cerebral Cortex, 25*(2), 406–414. https://doi.org/10.1093/cercor/bht231.

Mito, Y., Yoshida, K., Yabe, I., Makino, K., Hirotami, M., Tashiro, K., Kikuchi, S., & Sasaki, H. (2005). Brain 3D-SSP SPECT analysis in dementia with Lewy bodies, Parkinson's disease with and without dementia, and Alzheimer's disease. *Clinical Neurology and Neurosurgery, 107*(5), 396–403.

Mori, S., & van Zijl, P. C. M. (2002). Fiber tracking: Principles and strategies – A technical review. *NMR in Biomedicine, 15*, 468–480. https://doi.org/10.1002/nbm.781.

Mormina, E., Arrigo, A., Calamuneri, A., Granata, F., Quartarone, A., Ghilardi, M. F., Inglese, M., Di Rocco, A., Milardi, D., Anastasi, G. P., & Gaeta, M. (2015a). Diffusion tensor imaging parameters' changes of cerebellar hemispheres in Parkinson's disease. *Neuroradiology, 57*, 327–334. https://doi.org/10.1007/s00234-014-1473-5.

Mormina, E., Longo, M., Arrigo, A., Alafaci, C., Tomasello, F., Calamuneri, A., Marino, S., Gaeta, M., Vinci, S. L., & Granata, F. (2015b). Tractography of corticospinal tract and arcuate fasciculus in high-grade gliomas performed by constrained spherical deconvolution: Qualitative and quantitative analysis. *American Journal of Neuroradiology, 36*(10), 1853–1858. https://doi.org/10.3174/ajnr.A4368.

Morys, J., Bobinski, M., Wegiel, J., Wisniewski, H. M., & Narkiewicz, O. (1996). Alzheimer's disease severely affects areas of the claustrum connected with the entorhinal cortex. *Journal für Hirnforschung, 37*, 173–180.

Naghavi, H. R., Eriksson, J., Larsson, A., & Nyberg, L. (2007). The claustrum/insula region integrates conceptually related sounds and pictures. *Neuroscience Letters, 422*(1), 77–80.

Nasreddine, Z. S., Phillips, N. A., Bédirian, V., Phillips, N. A., Bèdirian, V., Charbonneau, S., Whitehead, V., Collin, I., Cummings, J. L., & Chertkow. (2005). The Montreal cognitive assessment, MoCA: A brief screening tool for mild cognitive impairment. *Journal of the American Geriatrics Society, 53*(4), 695–699.

Nombela, C., Rowe, J. B., Winder-Rhodes, S. E., Hampshire, A., Owen, A. M., Breen, D. P., Suncan, G. W., Khoo, T. K., Yarnali, A. J., Firbank, M. J., Chinnery, P. F., Robbins, T. W., O'Brien, J. T., Brooks, D. J., & Burn, D. J. (2014). Genetic impact on cognition and brain function in newly diagnosed Parkinson's disease: ICICLE-PD study. *Brain, 137*(Pt 10), 2743–2758. https://doi.org/10.1093/brain/awu201.

Ogomori, K., Kitamoto, T., Tateishi, J., Sato, Y., Suetsugu, M., & Abe, M. (1989). Beta-protein amyloid is widely distributed in the central nervous system of patients with Alzheimer's disease. *American Journal of Pathology, 134*, 243–251.

Parsons, M. W., Harrington, D. L., & Rao, S. M. (2005). Distinct neural systems underlie learning visuomotor and spatial representations of motor skills. *Human Brain Mapping, 24*(3), 229–247.

Pearson, R. C., Brodal, P., Gatter, K. C., & Powell, T. P. (1982). The organization of the connections between the cortex and the claustrum in the monkey. *Brain Research, 234*, 435–444.

Poewe, W. (2008). Non-motor symptoms in Parkinson's disease. *European Journal of Neurology, 15*(Suppl 1), 14–20. https://doi.org/10.1111/j.1468-1331.2008.02056.x.

Rektor, I., Svátková, A., Vojtíšek, L., Zikmundová, I., Vaníček, J., Király, A., & Szabó, N. (2018). White matter alterations in Parkinson's disease with normal cognition precede grey matter atrophy. *PLoS One, 13*(1), e0187939. https://doi.org/10.1371/journal.pone.0187939.

Remedios, R., Logothetis, N. K., & Kayser, C. (2014). A role of the claustrum in auditory scene analysis by reflecting sensory change. *Frontiers in Systems Neuroscience, 8*, 44. https://doi.org/10.3389/fnsys.2014.00044.

Roalf, D. R., Moberg, P. J., Xie, S. X., Wolk, D. A., Moelter, S. T., & Arnold, S. E. (2013). Comparative accuracies of two common screening instruments for classification of Alzheimer's disease, mild cognitive impairment, and healthy aging. *Alzheimer's & Dementia, 9*(5), 529–537. https://doi.org/10.1016/j.jalz.2012.10.001.

Roquet, D., Noblet, V., Anthony, P., Philippi, N., Demuynck, C., Cretin, B., Martin-Hunyadi, C., Loureiro de Sousa, P., & Blanc, F. (2017). Insular atrophy at the prodromal stage of dementia with Lewy bodies: A VBM DARTEL study. *Scientific Reports, 7*(1), 9437. https://doi.org/10.1038/s41598-017-08667-7.

Rubinov, M., & Sporns, O. (2010). Complex network measures of brain connectivity: Uses and interpretations. *NeuroImage, 52*, 1059–1069.

Selikhova, M., Williams, D. R., Kempster, P. A., Holton, J. L., Revesz, T., & Lees, A. J. (2009). A Clinico-pathological study of subtypes in Parkinson's disease. *Brain, 132*(11), 2947–2957. https://doi.org/10.1093/brain/awp234.

Shao, N., Yang, J., & Shang, H. (2015). Voxelwise meta-analysis of gray matter anomalies in Parkinson variant of multiple system atrophy and Parkinson's disease using anatomic likelihood estimation. *Neuroscience Letters, 587*, 79–86. https://doi.org/10.1016/j.neulet.2014.12.007.

Sherk, H., & LeVay, S. (1981). The visual claustrum of the cat. III. Receptive field properties. *Journal of Neuroscience, 1*(9), 993–1002.

Shima, K., Hoshi, E., & Tanji, J. (1996). Neuronal activity in the claustrum of the monkey during performance of multiple movements. *Journal of Neurophysiology, 76*(3), 2115–2119.

Shipp, S., Blanton, M., & Zeki, S. (1998). A visuo-somatomotor pathway through superior parietal cortex in the macaque monkey: Cortical connections of areas V6 and V6A. *European Journal of Neuroscience, 10*, 3171–3193.

Simuni, T., & Sethi, K. (2008). Nonmotor manifestations of Parkinson's disease. *Annals of Neurology, 64*(Suppl 2), S65–S80. https://doi.org/10.1002/ana.21472.

Smith, J. B., & Alloway, K. D. (2010). Functional specificity of claustrum connections in the rat: Interhemispheric communication between specific parts of motor cortex. *Journal of Neuroscience, 30*(50), 16832–16844. https://doi.org/10.1523/JNEUROSCI.4438-10.2010.

Smith, J. B., & Alloway, K. D. (2014). Interhemispheric claustral circuits coordinate sensory and motor cortical areas that regulate exploratory behaviors. *Frontiers in Systems Neuroscience, 8*, 93. https://doi.org/10.3389/fnsys.2014.00093.

Smythies, J. (2015). On the function of object cells in the claustrum—Key components in information processing in the visual system? *Frontiers in Cellular Neuroscience, 9*. https://doi.org/10.3389/fncel.2015.00443.

Smythies, J., Edelstein, L., & Ramachandran, V. (2012). Hypotheses relating to the function of the claustrum. *Frontiers in Integrative Neuroscience, 6*, 53. https://doi.org/10.3389/fnint.2012.00053.

Tanné-Gariépy, J., Boussaoud, D., & Rouiller, E. M. (2002). Projections of the claustrum to the primary motor, premotor, and prefrontal cortices in the macaque monkey. *The Journal of Comparative Neurology, 454*(2), 140–157.

Torgerson, C. M., & Van Horn, J. D. (2014). A case study in connectomics: The history, mapping, and connectivity of the claustrum. *Frontiers in Neoroinformatics, 8*, 83. https://doi.org/10.3389/fninf.2014.00083.

Torgerson, C. M., Irimia, A., Goh, S. Y., & Van Horn, J. D. (2015). The DTI connectivity of the human claustrum. *Human Brain Mapping, 36*(3), 827–838.

Tournier, J. D., Calamante, F., & Connelly, A. (2007). Robust determination of the fibre orientation distribution in diffusion MRI: Non-negativity constrained super-resolved spherical deconvolution. *NeuroImage, 35*(4), 1459–1472.

Tournier, J. D., Yeh, C. H., Calamante, F., Cho, K. H., Connelly, A., & Lin, C. P. (2008). Resolving crossing fibres using constrained spherical deconvolution: Validation using diffusion-weighted imaging phantom data. *NeuroImage, 42*(2), 617–625. https://doi.org/10.1016/j.neuroimage.2008.05.002.

Trzepacz, P. T., Hochstetler, H., Wang, S., Walker, B., & Saykin, A. J. (2015). Alzheimer's Disease Neuroimaging Initiative. Relationship between the Montreal cognitive assessment and mini-mental state examination for assessment of mild cognitive impairment in older adults. *BMC Geriatrics, 15*, 107. https://doi.org/10.1186/s12877-015-0103-3.

Van Eimeren, T., Monchi, O., Ballanger, B., & Strafella, A. P. (2009). Dysfunction of the default mode network in Parkinson disease: A functional magnetic resonance imaging study. *Archives of Neurology, 66*(7), 877–883. https://doi.org/10.1001/archneurol.2009.97.

Webster, M. J., Bachevalier, J., & Ungerleider, L. G. (1993). Subcortical connections of inferior temporal areas TE and TEO in macaque monkeys. *The Journal of Comparative Neurology, 335*(1), 73–91.

Yamamoto, R., Iseki, E., Murayamam, N., Minegishi, M., Marui, W., Togo, T., Katsuse, O., Kosaka, K., Kato, M., Iwatsubo, T., & Arai, T. (2007). Correlation in Lewy pathology between the claustrum and visual areas in brains of dementia with Lewybodies. *Neuroscience Letters, 415*, 219–224.

Yao, N., Shek-Kwan, C. R., Cheung, C., Pang, S., Lau, K. K., Suckling, H., Rowe, J. B., Yu, K., Ka-Fung, Mak. H., Chua, S., Ho, S. L., McAlonan, G. M. (2014). The default mode network is disrupted in Parkinson's disease with visual hallucinations. Human Brain Mapping, 35(11): 5658–5666. https://doi.org/10.1002/hbm.22577.